ATMOSPHERIC AND OCEANIC SCIENCE LETTERS, 2013, VOL. 6, NO. 5, 290–294

Interdecadal Variations of Winter Temperatures in East China During the Past 100 Years and Related Atmospheric Circulation

ZHU Ya-Li[1,2]

[1] *Nansen-Zhu International Research Centre, Institute of Atmospheric Physics, Chinese Academy of Sciences, Beijing 100029, China*
[2] *Climate Change Research Center, Chinese Academy of Sciences, Beijing 100029, China*

Received 8 October 2012; revised 20 November 2012; accepted 20 November 2012; published 16 September 2013

Abstract The winter temperature changes in East China during the past 100 years are investigated by using the Twentieth Century Version 2 (20th-v2) Reanalysis. Four typical warm (P1, 1911–30; P4, 1991–2010) and cold (P2, 1938–57; P3, 1961–80) periods are identified for the East China winter temperature index. Comparison of 160-station observational data, NCAR sea level pressure (SLP) data, and NCEP/NCAR Reanalysis shows that the 20th-v2 Reanalysis can successfully depict the major features of the warming from P3 to P4, which is part of the global warming phenomenon. The cooling from P1 to P2 is a regional phenomenon under global warming. However, both changes are consistent with the phase change of the Arctic Oscillation (AO), while the second change is also accompanied by the phase change of Antarctic Oscillation (AAO) from negative to positive. Original sources of the interdecadal shifts of the AO and winter temperature in East China require further research.

Keywords: East China, winter temperature, global warming, decadal change

Citation: Zhu, Y.-L., 2013: Interdecadal variations of winter temperatures in East China during the past 100 years and related atmospheric circulation, *Atmos. Oceanic Sci. Lett.*, **6**, 290–294, doi:10.3878/j.issn.1674-2834.12.0094.

1 Introduction

Global warming issues have been long debated by meteorologists and the public. An examination of climate variations during the past 100 years can provide more comprehensive information to help in understanding changes that occurred in the past several decades. However, because credible long-term observational climate data is not available, reanalysis and model output data can be used to study these climate changes.

As an important monsoon region, East China has experienced distinct interdecadal variations during the last 100 years such as the summer monsoon weakening after the late 1970s (Wang, 2001, 2002), summer precipitation increases (decreases) over the Huang-Huai River Valley (Yangtze River Valley) after late 1990s (Zhu et al., 2011), the winter monsoon weakening after the 1980s (Wang et al., 2009), and strengthened connection between winter temperature and Hadley circulation after the late 1970s (Zhou and Wang, 2008). Tang et al. (2009) have shown different time series of annual mean temperature averaged over China during past 100 years that correlate strongly and have consistent variations with global (Northern Hemisphere) mean temperature.

On the basis of observational temperature data from 160 stations reported by the National Climate Center of the China Meteorological Administration (CMA, http://www.cma.gov.cn/), the author used the cluster method to determine similarities in variations of winter temperatures recorded at stations in East China during 1951–2010. Thus, area-weighted winter temperature averaged over East China is studied in this paper. Although decadal changes in temperature in China during the last 100 years have been revealed (e.g., Tang et al., 2009), the related atmospheric circulations remain unclear. To investigate atmospheric circulation changes related to decadal temperature variations in East China, the Twentieth Century Version 2 (20th-v2) Reanalysis (2° latitude × 2° longitude) was employed to determine data as early as 1871. In addition, the National Centers for Environmental Prediction/the National Center for Atmospheric Research (NCEP/NCAR) Reanalysis (2.5° latitude × 2.5° longitude, Kalnay et al., 1996) and NCAR Northern Hemisphere sea level pressure (SLP) data from 1899 (5° latitude × 5° longitude, Trenberth and Paolino Jr, 1980) were used as reference data.

2 Results

Figure 1 shows the temperature indices (t_{index}) averaged over East China (25–43°N, 110–121°E , including 57 stations) on the basis of the 160-station data for 1951–2010 (black curve) and 20th-v2 Reanalysis for 1871–2010 (blue curve). The correlation coefficient between the two during 1951–2010 is 0.86:0.80 after the nine-year smoothed signals were removed and 0.95 after the nine-year signals were smoothed. Thus, the 20th-v2 Reanalysis, as a replacement of observational data, can provide valuable results for determining climate variations over East China during the past 100 years.

The running *t*-test was applied to examine the stability of the t_{index}. Two changing points were detected near the 1930s and 1980s by using different widths of windows such as 9, 11, 15, and 17 years. From the nine-year smoothed t_{index} (Figs. 1b and 1c), four typical periods were selected as 1911–30 (P1), 1938–57 (P2), 1961–80 (P3), and 1991–2010 (P4). These periods were divided into two sets; P1 and P2 represented typical warm and cold periods before 1960, and P3 and P4 represented typical cold and warm periods after 1961. The mean tem-

Corresponding author: ZHU Ya-Li, zhuyl@mail.iap.ac.cn

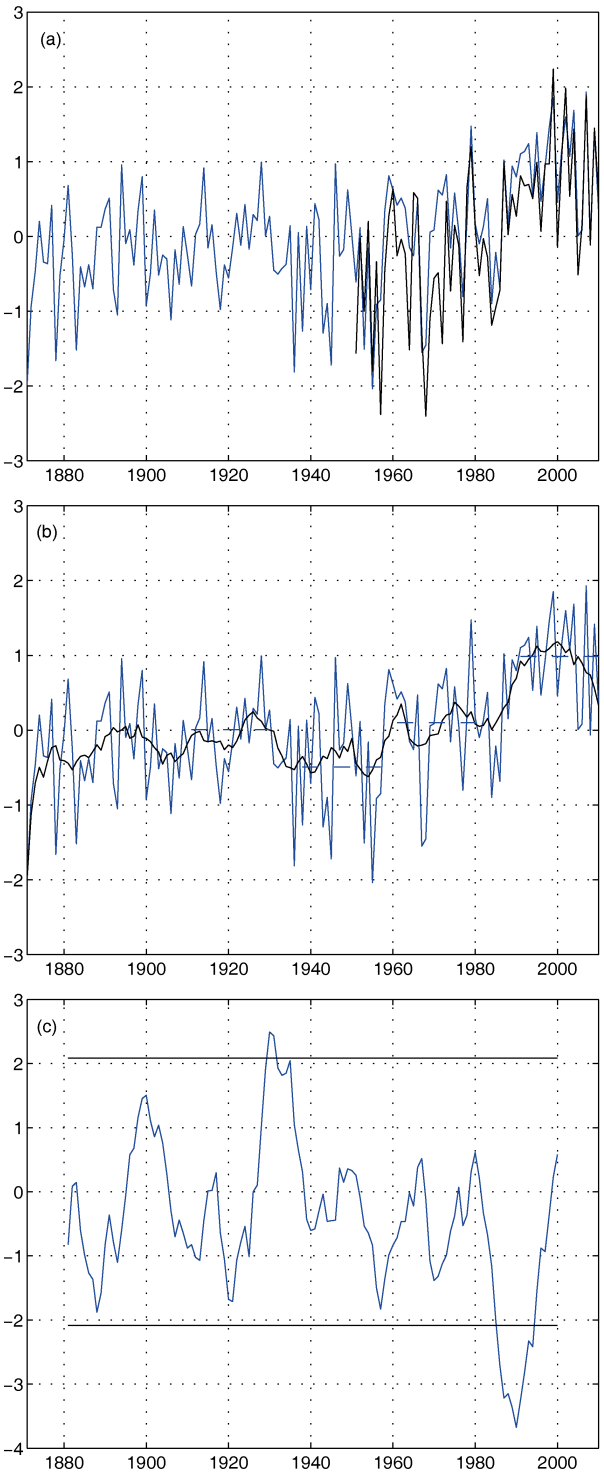

Figure 1 (a) Temperature indices (t_{index}) averaged over East China (25–43°N, 110–121°E) on the basis of 160-station data recorded during 1951–2010 (black curve) and Twentieth Century Version 2 (20th-v2) Reanalysis during 1871–2010 (blue curve). (b) t_{index} from 20th-v2; four typical warm/cold periods, P1 to P4 from left to right, are shown by dashed lines. (c) Running *t*-test of t_{index} from 20th-v2 with an 11-year window width showing *t* values of the index (blue curve) at the 95% confidence level (horizontal lines).

peratures for the four periods were 4.31°C, 3.56°C, 4.42°C, and 5.69°C, respectively.

To obtain a broader view of the temperature changes in the selected periods, differences in the global surface temperature at the 995 hPa level between the typical warm and cold periods (P4–P3 and P1–P2) are shown in Fig. 2. NCEP/NCAR Reanalysis reveals strong warming over the northern mid-high latitudes, particularly over Greenland and eastward; weaker warming over the low latitudes; and cooling over the southern high latitudes (Fig. 2c). The 20th-v2 Reanalysis also shows similar warming and cooling patterns, although the warming over the northern mid-high (low) latitudes are weaker (much stronger) than that shown by NCEP/NCAR Reanalysis (Fig. 2b). Although P1 was selected as a typical warm period for East China, this period shows surface temperatures lower than those in P2 over most areas with the exception of higher temperatures over most of the North Polar Region (Fig. 2a).

In the difference field of SLP, both NCAR SLP (in the data-covered area) and NCEP/NCAR reanalyses show patterns quite similar to those of the 20th-v2 Reanalysis

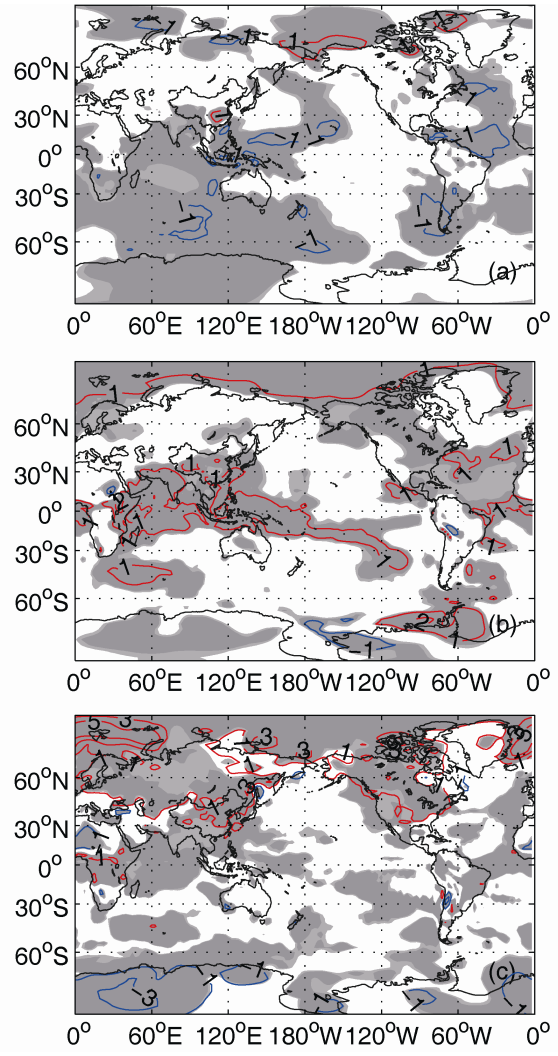

Figure 2 Differences in global surface temperature at 995 hPa level between (b, c) P4 and P3, and (a) P1 and P2. (a) and (b) are from the Twentieth Century Version 2 (20th-v2) Reanalysis; (c) is from the NCEP/NCAR Reanalysis. Contours represent the values of difference (blue, negative; red, positive), and shadings represent differences at the 90% and 95% confidence level derived through Student's *t*-test.

(Fig. 3) but with significantly larger magnitude over the globe. For P4–P3 (Figs. 3b, 3d, and 3e), negative (positive) values appear in the South/North Polar Region (southern/northern mid-latitudes), resembling a positive Antarctic/Arctic Oscillation (AAO/AO) pattern (Thompson and Wallace, 2000, 2001; Fan and Wang, 2004; Fan, 2007). In the difference field between P1 and P2 (Figs. 3a and 3c), negative values also occupy the North Polar Region, while large-scale positive values occupy the northern mid-latitudes (consistent in 20th-v2 and NCAR SLP) and southern mid-high latitudes. In addition, negative values exist in the eastern tropical Pacific.

Corresponding features appear at the 500 hPa geopotential height (Fig. 4). In the difference field between P4 and P3, NCEP/NCAR Reanalysis also shows changes over the globe similar to those shown in 20th-v2 data but with larger magnitude in the mid-low latitudes (Figs. 4b and 4c). Figure 4a reveals that negative values exist over the North Polar Region. For magnitude, the 20th-v2 Reanalysis shows significantly weaker changes over the globe at low levels than those shown in NCAR SLP and NCEP/NCAR reanalyses for P4–P3 (Figs. 2 and 3) but weaker/comparable changes in mid-low/high latitudes at high levels (Fig. 4). These results suggest more confidence in the 20th-v2 Reanalysis at high levels than that at low levels.

Figures 3 and 4 show that large-scale differences exist in the Polar Regions between typical warm and cold periods with anti-phase changes in the middle and high latitudes that resemble the AO and AAO patterns. Thus, the AO and AAO indices are calculated as the time series of the leading empirical orthogonal function component from the 20th-v2 SLP and are shown in Fig. 5. Correlation coefficients between AO/AAO and t_{index} are 0.34/0.26, at the 95% confidence level for the freedom degree of 140 (1871–2010) through Student's *t*-test and 0.5/0.67 after nine-year smoothing. The AO phases are consistent with the four typical periods with P1 and P4 showing positive AO and P2 and P3 showing negative AO; the AAO does not show phase change from P1 to P2.

3 Conclusion and discussion

Four typical warm (P1, 1911–30; P4, 1991–2010) and cold (P2, 1938–57; P3, 1961–80) periods were identified for the East China winter temperature index on the basis of the 20th-v2 Reanalysis. The differences in SLP and geopotential height field between typical periods from

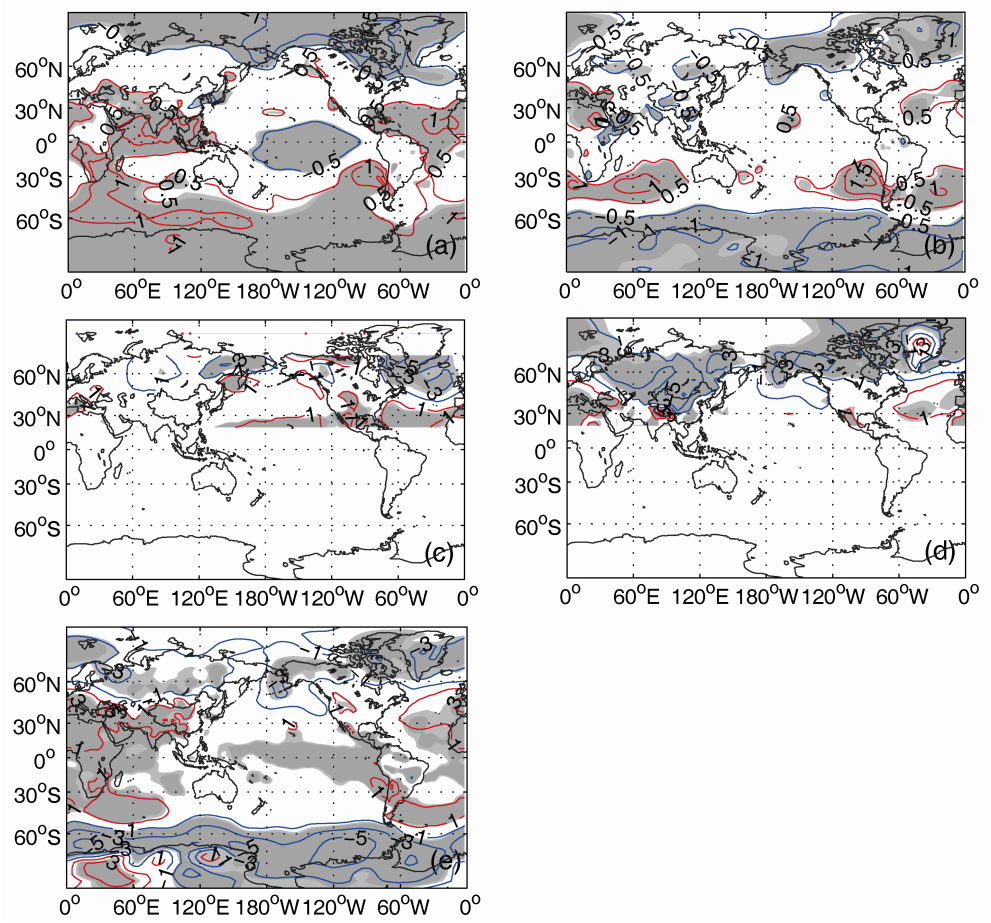

Figure 3 Differences in sea level pressure (SLP) between ((b), (d), and (e)) P4 and P3 and ((a) and (c)) P1 and P2. (a) and (b) are from the Twentieth Century Version 2 (20th-v2) Reanalysis; (c) and (d) are from the National Centers for Atmospheric Research (NCAR) SLP; and (e) is from the NCEP/NCAR Reanalysis. Contours represent the values of difference (blue, negative; red, positive), and shadings represent differences at the 90% and 95% confidence level derived through Student's *t*-test.

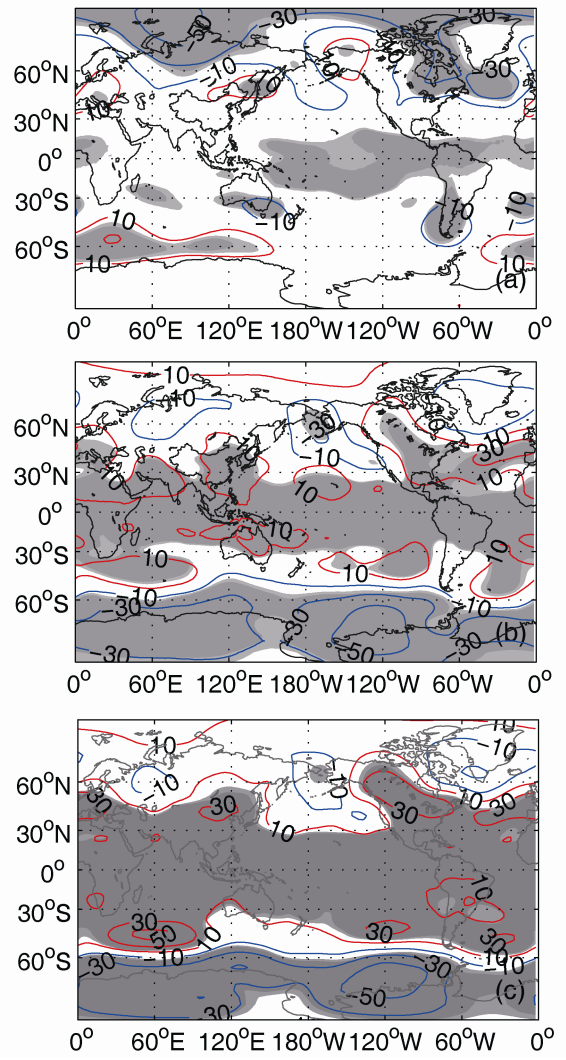

Figure 4 Differences in 500 hPa geopotential height between ((a), (c)) P4 and P3, and (b) P1 and P2. (a) and (b) are from the Twentieth Century Version 2 (20th-v2) Reanalysis; (c) is from the NCEP/NCAR Reanalysis. Contours represent the values of difference (blue, negative; red, positive), and shadings represent differences at the 95% confidence level derived through Student's *t*-test.

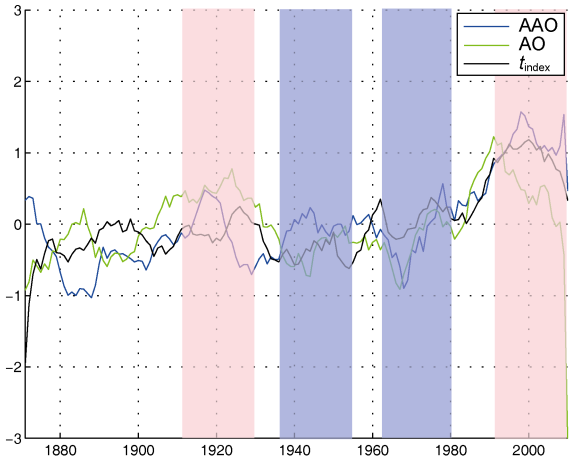

Figure 5 Standardized AO and AAO indices, and t_{index} after nine-year smoothing during 1871–2010. Typical warm and cold periods are shown by light red and blue shadows, respectively.

different datasets were investigated to reveal the atmospheric circulation features related to the temperature changes.

Compared with P3, most areas were warmer during P4, except for the southern high latitudes. The 20th-v2 Reanalysis depicted stronger differences in low latitudes and weaker differences in high latitudes than those shown by NCEP/NCAR. For SLP and 500 hPa geopotential height, three datasets revealed consistent difference patterns including negative values in southern and northern high latitudes and positive values in mid-low latitudes with weaker magnitude shown in the 20th-v2 data. However, as a typical warm period, P1 was characterized by colder climate than that in P2 over most areas with the exception of northern high latitudes. Negative values existed in northern high latitudes, and positive values occurred in northern mid-latitudes and southern mid-high latitudes. The changes from P1 to P2 and from P3 to P4 were synchronous with the phase changes of AO, which can be obviously detected from the variation of AO and East China temperature indices (Fig. 4). The change from P3 to P4 was also accompanied by the phase shift of AAO from negative to positive.

Winter temperatures in East China are closely connected with the East Asian winter monsoon (EAWM). Previous studies revealed that the AO can significantly affect the EAWM at the interannual timescale (Gong et al., 2001; Wu and Wang, 2002). These studies also suggest that the AO can influence EAWM directly through the impact on the SLP, East Asian trough, and surface air temperature and indirectly through influencing the Siberian High. Wang et al. (2009) investigated the significant weakening of the EAWM in late 1980s, which is consistent with the temperature changes from P3 to P4, and explained the phenomenon from a perspective of quasi-stationary planetary waves. Sun et al. (2008) and Sun and Wang (2012) revealed decadal variations in the relationship between summer North Atlantic Oscillation and the East Asian climate. However, the original sources of the interdecadal climate variations are quite complicated topics and require further exploration through both long-term data diagnosis and numerical simulations.

Acknowledgements. This work is supported jointly by the strategic technological program of the Chinese Academy of Sciences (Grant No. XDA05090405), the National Basic Research Program of China (Grant Nos. 2009CB421406 and 2010CB950304), and the Special Fund for the Public Welfare Industry (Meteorology; Grant Nos. GYHY201006022 and GYHY200906018).

References

Fan, K., 2007: Zonal asymmetry of the Antarctic Oscillation, *Geophys. Res. Lett.*, **34**, L02706, doi:10.1029/2006GL028045.

Fan, K., and H. Wang, 2004: Antarctic oscillation and the dust weather frequency in North China, *Geophys. Res. Lett.*, **31**, L10201, doi:10.1029/2004GL019465.

Gong, D. Y., S. W. Wang, and J. H. Zhu, 2001: East Asian winter monsoon and Arctic oscillation, *Geophys. Res. Lett.*, **28**, 2073–2076.

Kalnay, E., M. Kanamitsu, R. Kistler, et al., 1996: The NCEP/NCAR 40-Year reanalysis project, *Bull. Amer. Meteor. Soc.*, **77**,

437–471.

Sun, J., and H. Wang, 2012: Changes of the connection between the summer North Atlantic Oscillation and the East Asian summer rainfall, *J. Geophys. Res.*, **117**, D08110, doi:10.1029/2012JD 017482.

Sun, J., H. Wang, and W. Yuan, 2008: Decadal variations of the relationship between the summer North Atlantic Oscillation and middle East Asian air temperature, *J. Geophys. Res.*, **113**, D15107, doi:10.1029/2007JD009626.

Tang, G. L., Y. H. Ding, S. W. Wang, et al., 2009: Comparative analysis of the time series of surface air temperature over China for the last 100 years, *Adv. Climate Change Res.* (in Chinese), **5**, 71–78.

Thompson, D. W. J., and J. M. Wallace, 2000: Annular modes in the extratropical circulation. Part I: Month-to-month variability, *J. Climate*, **13**, 1000–1016.

Thompson, D. W. J., and J. M. Wallace, 2001: Regional climate impacts of the Northern Hemisphere annular mode, *Science*, **293**, 85–89.

Trenberth, K. E., and D. A. Paolino Jr, 1980: The Northern Hemisphere sea-level pressure data set: Trends, errors and discontinuities, *Mon. Wea. Rev.*, **108**, 855–872.

Wang, H. J., 2001: The weakening of Asian monsoon circulation after the end of 1970s, *Adv. Atmos. Sci.*, **18**, 376–386.

Wang, H. J., 2002: The instability of the East Asian summer monsoon-ENSO relations, *Adv. Atmos. Sci*, **19**, 1–11.

Wang, L., R. Huang, L. Gu, et al., 2009: Interdecadal variations of the East Asian winter monsoon and their association with quasi-stationary planetary wave activity, *J. Climate*, **22**, 4860–4872.

Wu, B., and J. Wang, 2002: Winter Arctic oscillation, Siberian high and East Asian winter monsoon, *Geophys. Res. Lett.*, **29**, 1897, doi:10.1029/2002GL015373.

Zhou, B. T., and H. J. Wang, 2008: Interdecadal change in the connection between Hadley circulation and winter temperature in East Asia, *Adv. Atmos. Sci*, **25**, 24–30.

Zhu, Y. L., H. J. Wang, W. Zhou, et al., 2011: Recent changes in the summer precipitation pattern in East China and the background circulation, *Climate Dyn.*, **36**, 1463–1473. doi:10.1007/s00382-010-0852-9.